energies

MDPI

Article

Applications of Machine Learning to Consequence Analysis of Hypothetical Accidents at Barakah Nuclear Power Plant Unit 1

Mohannad Khameis Almteiri and Juyoul Kim *

Department of NPP Engineering, KEPCO International Nuclear Graduate School, 658-91 Haemaji-ro, Seosaeng-myeon, Ulju-gun, Ulsan 45014, Korea
* Correspondence: jykim@kings.ac.kr; Tel.: +82-52-712-7306

Abstract: The United Arab Emirates (UAE) built four nuclear power plants at the Barakah site to supply 25% of the region's electricity. Among the Barakah Nuclear Power Plants, (BNPPs), their main objectives are to achieve the highest possible safety for the environment, operators, and community members; quality nuclear reactors and energy; and power production efficiency. To meet these objectives, decision-makers must access large amounts of data in the case of a nuclear accident to prevent the release of radioactive materials. Machine learning offers a feasible solution to propose early warnings and help contain accidents. Thus, our study aimed at developing and testing a machine learning model to classify nuclear accidents using the associated release of radioactive materials. We used Radiological Assessment System for Consequence Analysis (RASCAL) software to estimate the concentration of released radioactive materials in the four seasons of the year 2020. We applied these concentrations as predictors in a classification tree model to classify three types of severe accidents at Unit 1 of BNPPs each season. The average accuracy of the classification models in the four seasons was 97.3% for the training data and 96.5% for the test data, indicating a high efficacy. Thus, the generated classification models can distinguish between the three simulated accidents in any season.

Keywords: nuclear power plant; nuclear accident; machine learning; classification; regression

Citation: Almteiri, M.K.; Kim, J. Applications of Machine Learning to Consequence Analysis of Hypothetical Accidents at Barakah Nuclear Power Plant Unit 1. *Energies* **2022**, *15*, 6048. https://doi.org/10.3390/en15166048

Academic Editor: Dan Gabriel Cacuci

Received: 31 July 2022
Accepted: 19 August 2022
Published: 20 August 2022

1. Introduction

Sustainable energy production is a critical global challenge, with several conventional energy sources, such as coal-based power plants, posing a significant threat to people and the environment at large. Thus, there are intensifying efforts to transition to cleaner energy sources, such as nuclear power plants. Governments globally are extensively investing in these alternative energy production technologies to meet the present demand while protecting the environment and conserving resources for future generations. Nuclear power plants have proven reliable, partly because, when correctly managed, they are clean and have fewer negative environmental consequences than typical electrical power plants. Furthermore, nuclear reactors have a greater energy production capacity than many other alternative energy sources, such as hydro, wind, and solar power plants. However, the reactors have several problems, the most serious of which is the potential toxicity to the environment and people [1]. Public awareness of nuclear disaster prevention has grown following the Fukushima Daiichi Nuclear Power Plant accident. Early warning and detection of radioactive emissions in a nuclear accident are essential to guarantee the environment's safety, operators, and community members [2]. Notably, every accident type has a unique pattern that can support the analysis of its occurrence and the relevant mitigation measures [3]. A radiological consequence evaluation plan is also considered a vital element of a safety analysis procedure, mainly because it defines the safety parameters of a nuclear reactor. Ultimately, this process allows the design team to implement suitable measures to guarantee operators' well-being. In a severe nuclear accident, the protection action depends on the number of radioactive materials released and wind direction.

Recently, decision support systems (DSSs) have been observed as a key strategy for enhancing security and safety measures during emergency nuclear emergency operations. These tools support decision-makers in identifying accident patterns and taking appropriate protective steps. DSSs are particularly pivotal in the planning phase of the emergency response [4,5]. They are also highly connected to artificial intelligence, a technology that uses algorithms to produce accurate insights from amassed data. These attributes help reduce human error while dealing with nuclear reactors during anomalous situations at nuclear power plants. Hsieh et al. also report that DSSs minimize decision-making time by 25% and improve operators' decision-making accuracy by 18%, especially in the case of abnormal events in a power plant [6]. Furthermore, DSSs reduce the amount of information an operator should consider to make accurate decisions in dealing with anomalies at a power plant. This relevance motivated our study's use of a decision-making tree built from the Classification and Regression Tree (CART) model.

This study aimed to analyze the effects of radiation from a severe APR 1400 accident at Unit 1 of the Barakah Nuclear Power Plant (BNPP), the latest model of a nuclear reactor developed by South Korea. The study was based on simulation results obtained from various relevant computer applications. A model that can predict the type of occurring accident based on the radionuclides released into the environment was created. Notably, three hypothetical accidents on the BNPP were assumed for the study. Table 1 illustrates BNPP Unit 1 specifications.

Table 1. Specifications of Barakah unit 1.

Item	BNPP Unit 1
Location	Barakah, Abu Dhabi, UAE
Reactor type	PWR
Capacity	1400 MWe
Commercial operation	20 April 2021

2. Review of Previous Studies

Before introducing this study's proposed RASCAL model, reviewing some of the key alternatives available is vital. The following are some major substitutes that can be used for source term estimation and burnup calculations.

2.1. Source Term Estimation

2.1.1. Source Inversion Algorithms

All source inversion algorithms are essentially top-down techniques used to compute source terms. Due to their exceptional accuracy levels, these methods are favored over their bottom-down counterparts. In top-down systems, the atmospheric dispersion model of the solution to measurements is adjusted to approximate the source term. Moreover, to regularize the inverse problem, the source term's initial projections, often derived from bottom-up models, are utilized. A successful application of this approach in modeling nuclear disasters has been adequately documented by Kovalets et al. [7]. Due to their lack of real-time dimension, previous implementations were considered less effective. Therefore, Kovalets et al. created a source inversion algorithm that quantifies various models' time-dependent release rates using measurements at varying distances from the nuclear power plant (NPP) and gamma-dose rates (GDR). They tested their model in JRODOS, the European nuclear emergency response system, to validate it. According to their results, the model exhibits robustness and real-time applicability. The team incorporates meteorological data assimilation tools to maximize the source term's accuracy.

2.1.2. Inverse Modeling Tool

Saurier et al. also developed an inverse modeling technique for measuring the accidental atmospheric emission from an NPP [8]. Similar to most source inversion techniques,

their approach consolidates atmospheric dispersion models and environmental measurements to quantify the source term. Additionally, the method utilizes GDR measurements, where the source term's composition, σ, is reduced to the critical radionuclides' list. In order to optimize the selection of λ, the authors utilize the L-curve technique [8]. In particular, the maximum curve point is chosen from the graph of the source term versus J(σ) measures (residues). For every case that estimates the source term, the L-curve is used to compute a specific value of λ. Overall, inverse modeling is used to reconstruct the source terms and compute radionuclide composition. This approach is meticulous and suitable for the real-time reconstruction of the main release events, irrespective of the number of measurements available.

2.1.3. Kalman Filter-Based Approach

Di Ronco and Cammi propose an improved backward method, which is fundamentally an adapted Kalman filter-based technique. The Kalman filter is a data simulation algorithm, initially visualized as an iterative predictive-corrector state estimator [9]. Di Ronco and Cammi incorporate the Gaussian plume dispersion algorithm into the Kalman filter to build their online data simulation tool. The resultant model implements online updates of approximated quantities by comparing measurements with model predictions. Furthermore, by exploiting the most recent unknown parameters' projections, the algorithm can determine mobile sensors' feasible placements [9]. A simulation loop depicts three details: (1) the current parameter estimates, (2) the sensor's current location, and (3) measurement estimations. Contrastingly, the control loop controls the sensor depending on current parameter estimates. In order to quantify the experimental observations' role throughout estimate updates, sensor noise level data is leveraged. Ultimately, the tool applies to single-source, steady-state situations that obey the Gaussian plume model.

2.1.4. Forward-Backward Coupled Estimation

A coupled source term estimation model is proposed by Sun, Fang, and Li [10]. Generally, to project source terms, backward techniques relying on environmental monitoring data or forward methods utilizing an NPP's status data are used. Both approaches comprise considerable uncertainties capable of compromising the results' accuracy. Therefore, for a more precise estimation, Sun et al. advocate for a forward-backward coupled approach [10]. In this instance, the Response Technical Manual (RTM-96) and the ensemble Kalman filter act as the forward and backward tools, respectively. In order to minimize the backward component's temporal correlation of estimates, the combined system uses the forward estimate's evolution model [10]. This consolidated process reduces the proliferation of uncertainties. Sun et al. conducted numerical and sensitivity assessments using the combined technique to reinforce the model's accuracy and robustness using a hypothetical NPP accident. Therefore, the RTM-96-ensemble Kalman filter model is practical for real-time estimating the source term in modern NPPs.

2.1.5. Grey Wolf Optimizer Algorithm and the Corrected Gaussian Diffusion Model

Another combined tool for rapidly estimating the source term is proposed by Liu et al. [11]. Their Grey Wolf Optimizer (GWO) is merged with the Gaussian diffusion model to improve the computation of the source term. Markedly, the Gaussian plume represents the diffusion model, while gas concentrations at various stations are calculated using the plume height, distance deviation coefficient, wind speed, and emission source strength [11]. Contrastingly, the GWO is used for solving the objective function. It is a swarm intelligence algorithm derived from the wolf pack's prey predation and class system [11]. In this model, the fittest, second-best, and third-best refer to the parameters α, β, and δ, respectively. The other potential solutions, ω, conform to the three classes of wolves. Such a conceptualization accounts for the GWO's ability to compute the source term reliably and rapidly. The Gaussian model is incorporated into the model using a terrain correction factor to optimize

accuracy. This case further demonstrates the essence of source estimation tools that utilize amalgamated approaches.

2.2. Recently Developed Methods for Burnup Calculations

2.2.1. Trajectory Period Folding Method

The Trajectory Period Folding (TPF) approach can be feasibly utilized to model nuclear transformations numerically. The basis of the technique is the linear chain method, often utilized for modeling isotropic changes in matter [12]. Based on Stanisz, Oettingen, and Cetnar's description, to build linear chain depictions, TPF folds in two successive periods [12]. Over the cumulative period of interest, what is considered is the linear nuclide-to-nuclide mass flow of transitions following each phase's creation of nuclide transmutation chains. This approach promotes the retention of all quantitative data detailing the isotropic transformation for the time-lapse beyond a given computation step [12]. Moreover, from the start of irradiation to a random time step, the evaluation of an isotope's history is facilitated by TPF. Cooling periods for all nuclear cycles and multi-recycling are included in this capability. Furthermore, TPF can safely detail the reactions that frequently proceed in nuclide production. Therefore, TPF creates a roadmap for rapid and accurate burnup calculations.

2.2.2. Serpent-SUBCHANFLOW-TRANSURANUS

To conduct pin-by-pin burnup computations, Garcia et al. propose a simulation tool based on Serpent 2, SUBCHANFLOW (SCF), and TRANSURANUS (TU) [13]. The technique consolidates fuel-performance analysis, Monte Carlo neutron transport, and subchannel thermal hydraulics to simulate depletion in a highly detailed manner. The method can be used to quantify burnup-dependent safety variables at the pin levels for various designs of NPPs [12]. Markedly, an object-oriented setup featuring a mesh-feedback exchange is the basis for the Serpent–SCF–TU coupling system [13]. Serpent 2's novel Collision-based Domain Decomposition (CDD) scheme spreads burnable materials across computation nodes, facilitating large-scale burnup calculations. In particular, this technique defines fields with only the related data and a fraction of the combustible materials, while replicating the rest of the model data in other domains [13]. Thanks to this system, it is possible to derive solutions to problems that cannot be accommodated by one node. Therefore, the Serpent–SCF–TU pin-by-pin burnup computations are sufficiently detailed and accurate.

3. Materials and Methods

3.1. Accident Scenarios

Loss of Coolant Accident (LOCA) is a simulated accident involving the loss of the core cooling system. Consequently, there is an automated actuation of the safety injection system (SIS) to keep the reactor core cooled and submerged. For this study, it was simulated that the SIS was disabled while, at the same time, the coolant was discharged through a break. Therefore, there was neither a cooling water injection nor an instantaneous trip of the reactor. Due to the rapid depressurization, the core was uncovered for a few seconds. Subsequently, there was a rapid increase in the fuel temperature, and the interaction between steam and the cladding was fastened. After the core was uncovered for a short while, the reactor began to melt. In this accident, different ranges of power 100%, 70%, 50%, and 20% are analyzed under the condition of LOCA with the ability to use a spray system on/off once the release becomes on the containment. The accident started at 00:00 (midnight), and the core was uncovered at 05:00. The release rate was 0.3 per day, and the operators could not save the core from melting down. It was assumed that the release was inside the containment.

Long Term Station Blackout (LTSBO) is an accident involving the total loss of electric energy in the Barakah nuclear power plant. Essentially, it was modeled that both onsite and offsite emergency systems were lost in the power plant. The trip signals for the reactors

were generated due to the low coolant flow level. Consequently, there was an accelerated increase in reactor pressure, which further caused an increase in reactor coolant temperature. Since there were no steam flows due to stopped feed-water pumps, the increased pressure was slowly discharged through the main steam safety valves (MSSVs). Despite shutting down the reactor and stopping the chain reactions through control elements, the coolant temperature continued to grow due to the increased decay heat. Similarly, there was a continued pressure increase until the pilot-operated safety relief valve opened. This scenario enabled the release of excess pressure. Despite the pilot-operated safety relief valve opening to release extra pressure, the reactors' coolant continued heat-up, which led to further heat transfer to the steam generator since the feed-water systems were stopped. This situation led to a maintained high reactor pressure that sustained the opening of the relief valve. The resultant effect was a decreased volume of the reactors' liquid as the reactor core remained uncovered. In this study, we assumed that the site lost power for a long period, between 8 to 12 h. The reactor shutdown event was at 00:00 (midnight), and the release from the core started on the same day at noon. The accident was tested with both systems spray on/off. The operators could not save the core from melting down, and the release pathway was inside the containment.

Steam Generator Tube Rupture (SGTR) is an accident that occurred simultaneously when the plant experienced a power blackout. The APR 1400 reactors have the potential to withstand this accident. The rupture of the steam generator tube (double-ended U-tube in that case) resulted in the reactors' tripping with immediate turbine tripping at a high level. There was no assumption of time delay between the power blackout occurrence and the steam generator tube rupture. This rupture can lead to leakage of Radionuclides from the primary to the secondary side. This study used a different range of powers of 100%, 70%, 50%, and 20% with this accident. The shutdown occurred at 00:00 (midnight), the leak rate into the steam generator was 500 gal/min, and the rupture location was above water level. The condenser was exhausted at 06:00 after activation of the safety relief valve. In this case of an accident, the release pathway would be to the steam generator.

3.2. Accident Assessment

The accident assessment was divided into three phases and illustrated in Figure 1.

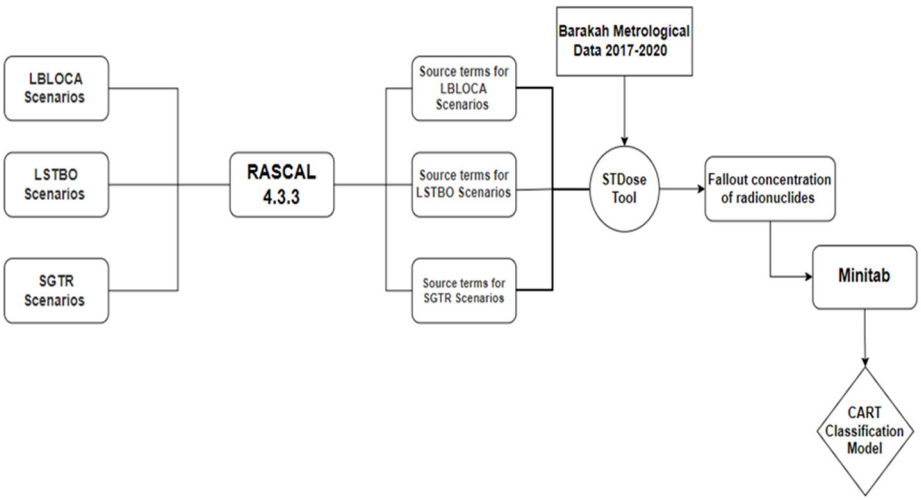

Figure 1. Schematic approach for methodology and analysis.

1. The first phase involved using Radiological Assessment System for Consequence Analysis (RASCAL) to generate the radiological source terms for each of the three accidents at the APR 1400 power plant.
2. The second phase involved using the source term to dose tool (STDose) of RASCAL to estimate the fallout concentration of radionuclides for each of the three accidents analyzed.

3. The third phase involved building a decision tree model using CART® classification based on the estimated radionuclides concentration.

3.3. RASCAL

RASCAL version 4.3.3 software was developed to rapidly estimate doses from nuclear or radiological emergencies, helping the decision-making process during the implementation of protective actions such as evacuation and sheltering in the first four days after a nuclear accident [14]. This study used RASCAL to generate the radiological source terms for each of the three accidents at the APR 1400 power plant. The STDose in RASCAL was used to estimate radiation doses from plumes to people downwind. STDose required information such as event location, event type, release path, source term, and meteorological data. The meteorological data were used to evaluate the atmospheric dispersion and transport model of radioactive effluents released from the Barakah Nuclear Power Plant weather station. To fulfill RASCAL requirements, five days were taken from each season as follows:

- Winter: 1–5 January 2020
- Spring: 1–5 April 2020
- Summer: 1–5 August 2020
- Fall: 1–5 October 2020

The National Center of Meteorology (NCM) in the United Arabs Emirates collected the meteorological data for these five days. Notably, RASCAL can only perform simulations for 96 h, informing the choice of the number of days. The STDose tool will first generate a time-dependent "source term." The source terms were input to an atmospheric dispersion and transport model. The atmospheric dispersion and transport model estimates radionuclide concentrations downwind in the air and ground due to deposition. The dose pathways are cloud shine from the plume, inhalation from the plume, and ground shine from deposited radionuclides (assuming four days of exposure to ground shine). Gaussian plume and Gaussian puff models are embedded within RASCAL for the atmospheric transport, dispersion, and deposition of radioactive materials from the release point. A simplified version of the straight-line Gaussian model is expressed as:

$$\frac{X(x,y,z)}{Q} = \frac{1}{(2\pi)^{\frac{3}{2}}\sigma_x\sigma_y\sigma_z} exp\left[\frac{-1}{2}\left(\frac{x-x_0}{\sigma_x}\right)^2\right] \times exp\left[\frac{-1}{2}\left(\frac{y-y_0}{\sigma_y}\right)^2\right] \times exp\left[\frac{-1}{2}\left(\frac{z-z_0}{\sigma_z}\right)^2\right] \quad (1)$$

where χ is the concentration (Bq/m^3 or g/m^3), Q is the amount of material unconfined (Bq or g), and σ is the dispersion parameter (m), which is a function of distance from the release point.

3.4. CART (Classification and Regression Tree) Model

The CART® classification is a supervised machine learning algorithm that uses historical data to construct a prediction model in a decision tree [15]. Typically, a decision tree is an upside-down tree-like diagram with the root node at the top, multiple internal nodes, and several terminal nodes at the bottom. Data are passed through a series of splits, called nodes, at which a decision is made about which direction to proceed based on one of the explanatory variables [16]. The goal is to get a predicted class at the terminal node. Because the CART model is a nonparametric model that does not make any assumptions about the mapping function between outcome and predictors, they are free to learn any functional form from the training data. However, the CART model requires more training datasets than parametric methods, such as Naive Bayes [17]. This limitation was overcome by using big data and simulating multiple accidents at varying power levels with different safety parameters. The algorithm chooses the variable and its split point that most reduces the root or parent node impurity. It then assigns classes to these nodes according to a rule that minimizes misclassification costs [18]. A node's misclassification cost is the proportion of observations that do not belong to the majority class in that node [19]. In our model, training is conducted on 70% of the data using Gini's index for node splitting [15]. The

optimal tree was the smallest tree with a misclassification cost within one standard error of the tree with the minimum misclassification cost. A total of 30% of the data were used to test the performance of the trained model to improve the generalizability of the trained model.

3.5. Data Generation

Only three radionuclides (^{137}Cs, ^{131}I, and ^{133}Xe) were selected as predictors in our model, based on previous severe accident data from Chernobyl and Fukushima. In addition, these three radionuclides had long half-lives (Table 2), which enabled multiple sampling. The fallout concentration of these three radionuclides was used as the input data for the CART model. The final sampled data consisted of 7700 rows for each season/month (Winter/January, Spring/April, Summer/August, and Fall/October), generating the big data preferred in predictive modeling. Each season/month data was used to train and test a decision tree model using the same criteria listed above (70%/30% train/test; Gini's index for node splitting; the optimal tree was the smallest tree with a misclassification cost within one standard error of the tree with the minimum misclassification cost).

Table 2. Selected radionuclides.

Radionuclides	Half-Life
^{137}Cs	30.17 years
^{131}I	8.0197 days
^{133}Xe	5.245 years

4. Results

4.1. Variable Importance

The ranking of predictors that classify the three accidents is shown as a bar graph (Figures 2–5). The predictors' ranking was similar across three months, August-summer, Winter-January, and Fall-October, with I-131 the most important, followed by Cs-137 and Xe-133. For April (spring), Cs-137 was the most important, followed by I-131 and Xe-133.

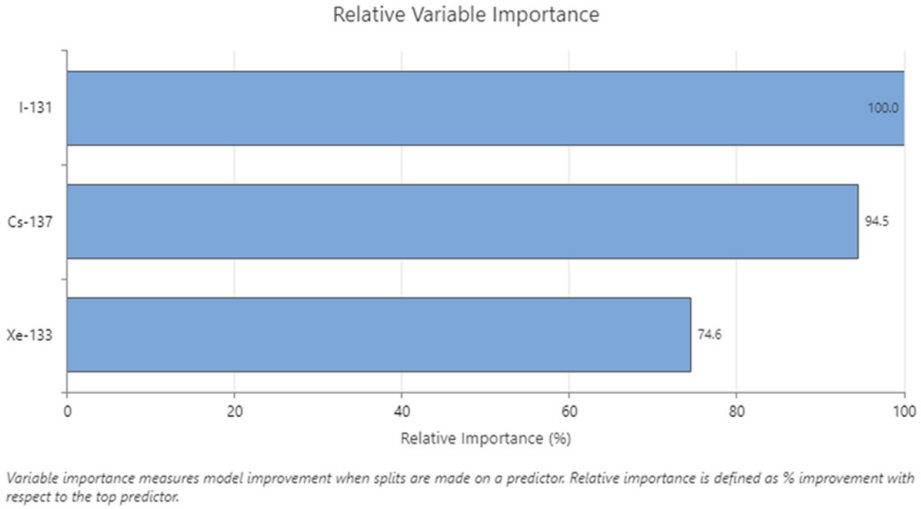

Figure 2. Graph showing the relative importance of the predictors for August (summer).

4.2. Accuracy

Focusing on the test data as a measure of model performance, the LOCA accident was best predicted in Spring April (97.3% accuracy) and least predicted in Winter January (84.0% accuracy). On the other hand, the LTSBO accident was best predicted in Summer August (98.8% accuracy) and least predicted in Winter January (97.4% accuracy). Finally, the SGTR accident was best predicted in Spring-April or Fall-October (99.4% accuracy for

both) and least predicted in Summer August or Winter January (99.2% accuracy for both). The overall accuracy for the three accidents in the test data was best in Summer August (98.0% accuracy), followed by Spring April (97.9% accuracy), Fall October (97.7% accuracy), and finally, Winter January (92.5% accuracy), as shown in Table 3.

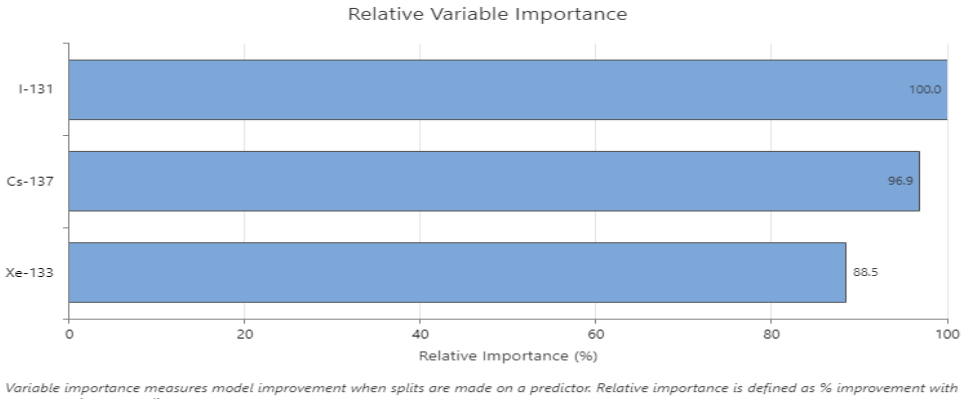

Figure 3. Graph showing relative importance of predictors in January (winter).

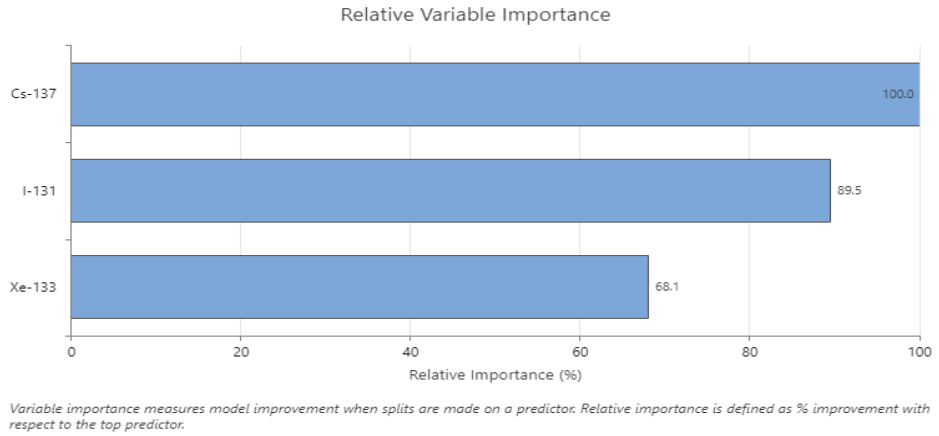

Figure 4. Graph showing relative importance of predictors April (spring).

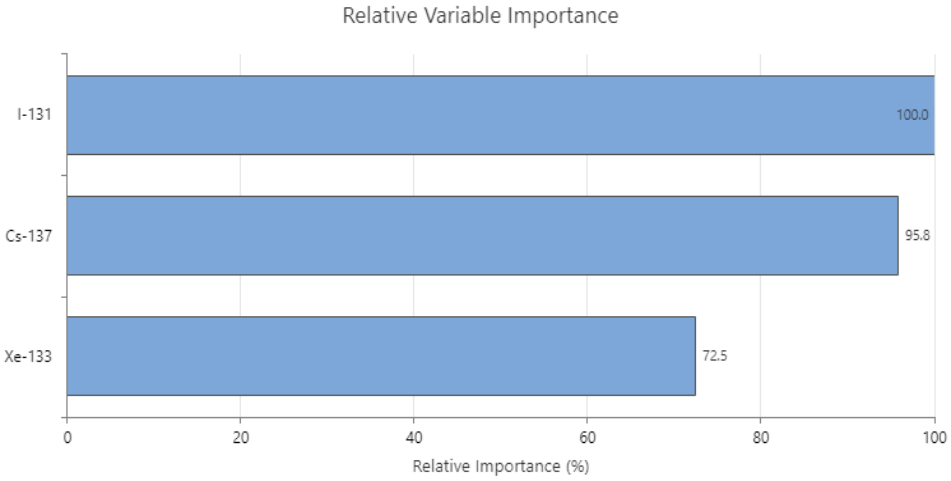

Figure 5. The relative importance of predictors in October (fall).

Table 3. The accuracy of the four models tested.

Accuracy	Summer August	Winter January	Spring April	Fall October
LOCA (train)	98.5%	84.7%	98.1%	97.4%
LOCA (test)	96.6%	84.0%	97.3%	96.0%
LTSBO (train)	99.3%	98.3%	98.0%	98.8%
LTSBO (test)	98.8%	97.4%	97.8%	98.5%
SGTR (train)	99.9%	99.5%	99.9%	99.9%
SGTR (test)	99.2%	99.2%	99.4%	99.4%
Overall (train)	99.1%	93.1%	98.4%	98.4%
Overall (test)	98.0%	92.5%	97.9%	97.7%

4.3. ROC AUC

The receiver operator characteristic (ROC) curve with its area under the curve (AUC) is another metric for evaluating the four models' performance in correctly classifying each accident. ROC AUC is the probability that the classification model ranks a random positive for a specific accident [1]. Generally, the classification of the four models for each accident type was excellent and never went below 0.97. Focusing on the test data, the LOCA accident had the best ROC AUC in Spring April (AUC = 0.9892) and least AUC in Winter January (AUC = 0.9752). The LTSBO accident had the best AUC in Spring April (AUC = 0.9921) and the least AUC in Winter January (AUC = 0.9768). The SGTR accident had the best AUC in Spring April or Fall October (AUC = 0.9989 for both) and least AUC in Winter January (AUC = 0.9979), as shown in Table 4.

Table 4. ROC AUC of the three accidents in the four models tested.

ROC AUC	Summer August	Winter January	Spring April	Fall October
LOCA (train)	0.9987	0.9800	0.9956	0.9952
LOCA (test)	0.9888	0.9752	0.9892	0.9846
LTSBO (train)	0.9985	0.9802	0.9953	0.9951
LTSBO (test)	0.9920	0.9768	0.9921	0.9860
SGTR (train)	0.9994	0.9991	0.9991	0.9991
SGTR (test)	0.9985	0.9979	0.9989	0.9989

5. Discussion and Conclusions

The research demonstrated that offsite parameters could support prompt decision-making during a nuclear disaster when onsite parameters are unavailable [1]. In this case, machine learning is a viable option for the underlying assessments. This study also noted the significance of using released radioactive materials to identify and categorize nuclear power plant accidents. Specifically, the radioactive materials released to the environment were used to identify and classify the three scenarios/accidents: LOCA with spray on/off, LSTBO with spray on/off, and SGTR without spray on/off. The three accidents were categorized at level seven on the International Nuclear and Radiological Event Scale (INES), meaning that significant radioactive materials were emitted. These discharges are associated with health and environmental consequences that necessitate public protective actions. Using the RASCAL 4.3.3 output, a machine learning model was developed for each season/month using the Minitab analysis software. The average accuracy of the classification model across the four seasons was 97.3% for the training data and 96.5% for the test data. The accuracy values were high, although they decreased slightly in Winter/January, indicating that the classification model could potentially categorize the accidents based on the radioactive materials released. These findings demonstrate that the radionuclides released at a specific time can help predict the accident type that might occur in the nuclear power plant. Thus, the study succeeded in developing and testing a machine learning model to classify nuclear accidents using the associated release of radioactive materials. The obtained results were contingent on several factors that affected the accuracy. Firstly, the classification model's accuracy increased with the volume of big

data accumulated. Secondly, seasonal variations impacted the prediction outcomes, with the lowest accuracy reported during winter. Future research should focus on developing optimization approaches to eliminate the effects of seasonal variability, which may be significant in different geographical locations. Furthermore, research is needed to outline the most informative metrics for predicting the concentration of radioactive materials. Notwithstanding, the findings of our study were adequately accurate and significant.

Author Contributions: Conceptualization, M.K.A. and J.K.; methodology, M.K.A.; software, M.K.A.; validation, J.K.; formal analysis, M.K.A.; investigation, M.K.A. and J.K.; resources, M.K.A. and J.K.; data curation, M.K.A.; writing-original draft preparation, M.K.A.; writing—review and editing, J.K.; visualization, M.K.A.; supervision, J.K.; project administration, J.K.; funding acquisition, J.K. All authors have read and agreed to the published version of the manuscript.

Funding: This work was supported by the Nuclear Safety Research Program through the Korea Foundation of Nuclear Safety (KoFONS) using the financial resource granted by the Nuclear Safety and Security Commission (NSSC) of the Republic of Korea (No. 2003015). This research was also supported by the 2022 Research Fund of the KEPCO International Nuclear Graduate School (KINGS), the Republic of Korea.

Institutional Review Board Statement: Not applicable.

Informed Consent Statement: Not applicable.

Data Availability Statement: The data that support the findings of this study are available on request from the corresponding author.

Conflicts of Interest: The authors declare no conflict of interest.

References

1. El-Hameed, A.A.; Juyoul, K. Machine Learning-Based Classification and Regression Approach for Sustainable Disaster Management: The Case Study of APR1400 in Korea. *Sustainability* **2021**, *13*, 9712. [CrossRef]
2. Ling, Y.; Yue, Q.; Huang, T.; Shan, Q.; Hei, D.; Zhang, X.; Jia, W. Multi-Nuclide Source Term Estimation Method for Severe Nuclear Accidents from Sequential Gamma Dose Rate Based on a Recurrent Neural Network. *J. Hazard. Mater.* **2021**, *414*, 125546. [CrossRef] [PubMed]
3. dos Santos, M.C.; Pinheiro, V.H.C.; do Desterro, F.S.M.; de Avellar, R.K.K.; Schirru, R.; dos Santos Nicolau, A.; de Lima, A.M.M. Deep Rectifier Neural Network Applied to the Accident Identification Problem in a PWR Nuclear Power Plant. *Ann. Nucl. Energy* **2019**, *133*, 400–408. [CrossRef]
4. Sweeck, L.; Camps, J.; Mikailova, R.; Almahayni, T. Role of Modelling in Monitoring Soil and Food During Different Stages of a Nuclear Emergency. *J. Environ. Radioact.* **2020**, *225*, 106444. [CrossRef] [PubMed]
5. Malizia, A.; Carestia, M.; Cafarelli, C.; Milanese, L.; Pagannone, S.; Pappalardo, A.; Pedemonte, M.; Latini, G.; Barlascini, O.; Fiorini, E. The Free License Codes as Decision Support System (DSS) for the Emergency Planning to Simulate Radioactive Releases in Case of Accidents in the New Generation Energy Plants. *WSEAS Trans. Environ. Dev.* **2014**, *10*, 453–464.
6. Hsieh, M.-H.; Hwang, S.-L.; Liu, K.H.; Liang, S.-F.M.; Chuang, C.-F. A Decision Support System for Identifying Abnormal Operating Procedures in a Nuclear Power Plant. *Nucl. Eng. Des.* **2012**, *249*, 413–418. [CrossRef]
7. Kovalets, I.; Andronopoulos, S.; Hofman, R.; Seibert, P.; Ievdin, I. Advanced Method for Source Term Estimation and Status of its Integration in JRODOS. *Radioprotection* **2016**, *51*, S121–S124. [CrossRef]
8. Saunier, O.; Korsakissok, I.; Didier, D.; Doursout, T.; Mathieu, A. Real-time Use of Inverse Modeling Techniques to Assess the Atmospheric Accidental Release of a Nuclear Power Plant. *Radioprotection* **2020**, *55*, 107–115. [CrossRef]
9. Di Ronco, A.; Giacobbo, F.; Cammi, A. A Kalman Filter-Based Approach for Online Source-Term Estimation in Accidental Radioactive Dispersion Events. *Sustainability* **2020**, *12*, 10003. [CrossRef]
10. Sun, S.; Li, H.; Fang, S. A Forward-Backward Coupled Source Term Estimation for Nuclear Power Plant Accident: A Case Study of Loss of Coolant Accident Scenario. *Ann. Nucl. Energy* **2017**, *104*, 64–74. [CrossRef]
11. Liu, Y.; Jiang, Y.; Zhang, X.; Pan, Y.; Qi, Y. Combined Grey Wolf Optimizer Algorithm and Corrected Gaussian Diffusion Model in Source Term Estimation. *Processes* **2022**, *10*, 1238. [CrossRef]
12. Stanisz, P.; Mikołaj, O.; Jerzy, C. Development of a Trajectory Period Folding Method for Burnup Calculations. *Energies* **2022**, *15*, 2245. [CrossRef]
13. García, M.; Vočka, R.; Tuominen, R.; Gommlich, A.; Leppänen, J.; Valtavirta, V.; Imke, U.; Ferraro, D.; Van Uffelen, P.; Milisdörfer, L.; et al. Validation of Serpent-SUBCHANFLOW-TRANSURANUS Pin-by-Pin Burnup Calculations using Experimental Data from the Temelín II VVER-1000 Reactor. *Nucl. Eng. Technol.* **2021**, *53*, 3133–3150. [CrossRef]
14. RASCAL 4: Description of Models and Methods. Available online: https://www.nrc.gov/docs/ML1303/ML13031A448.pdf (accessed on 1 November 2021).

15. Timofeev, R. Classification and Regression Trees (CART) Theory and Applications. Master's Thesis, Humboldt University, Berlin, Germany, 2004.
16. Moisen, G.G. Classification, and Regression Trees. In *Encyclopedia of Ecology*; Jorgensen, S.E., Fath, B.D., Eds.; Elsevier: Oxford, UK, 2008; p. 582.
17. Ghiasi, M.M.; Zendehboudi, S.; Mohsenipour, A.A. Decision Tree-Based Diagnosis of Coronary Artery Disease: CART Model. *Comput. Methods Programs Biomed.* **2020**, *192*, 105400. [CrossRef] [PubMed]
18. Minitab Software for Quality Improvement. Available online: https://www.minitab.com/en-us/ (accessed on 1 November 2021).
19. Alin, A. Minitab. *WIREs Comput. Stat.* **2010**, *2*, 723–727. [CrossRef]